

A double detached shell around a post-Red Supergiant: IRAS 17163-3907, the Fried Egg nebula $\star, \star\star$

E. Lagadec¹, A.A. Zijlstra², R.D. Oudmaijer³, T. Verhoelst⁴, N.L.J. Cox⁴, R. Szczerba⁵, D. Mékarnia⁶ and H. van Winckel⁴

¹ European Southern Observatory, Karl Schwarzschildstrasse 2, Garching 85748, Germany

² Jodrell Bank Center For Astrophysics, The University of Manchester, School of Physics & Astronomy, Manchester M13 9PL, UK

³ School of Physics and Astronomy, University of Leeds, Leeds LS2 9JT, UK

⁴ Instituut voor Sterrenkunde, K.U. Leuven, Celestijnenlaan, 200D, 3001, Leuven, Belgium

⁵ N. Copernicus Astronomical Center, Rabiańska 8, 87-100 Toruń, Poland

⁶ Lab. H. Fizeau, CNRS UMR 6525, Univ. de Nice-Sophia Antipolis, Observatoire de la Côte d'Azur, 06108 Nice, France

Received ; accepted

ABSTRACT

Context. We performed a mid-infrared imaging survey of evolved stars in order to study the dust distribution in circumstellar envelopes around these objects and to better understand the mass-loss mechanism responsible for the formation of these envelopes. During this survey, we resolved for the first time the circumstellar environment of IRAS 17163-3907 (hereinafter IRAS17163), which is one of the brightest objects in the mid-infrared sky, but is surprisingly not well studied.

Aims. Our aim is to determine the evolutionary status of IRAS 17163 and study its circumstellar environment in order to understand its mass-loss history.

Methods. We obtained diffraction-limited images of IRAS 17163 in the mid-infrared using VISIR on the VLT. Optical spectra of the object allowed us to determine its spectral type and estimate its distance via the presence of diffuse interstellar bands.

Results. We show that IRAS 17163 is a Post-Red Supergiant, possibly belonging to the rare class of Yellow Hypergiants, and is very similar to the well studied object IRC +10420. Our mid-infrared images of IRAS 17163 are the first direct images of this bright mid-infrared source. These images clearly show the presence of a double dusty detached shell around the central star, due to successive ejections of material with a timescale of the order of 400 years and a total circumstellar mass larger than $4 M_{\odot}$. This indicates that non quiescent mass-loss occurs during this phase of stellar evolution.

Key words. circumstellar matter – Stars: mass-loss – (Stars:) supergiants – Infrared: stars

1. Introduction

After exhausting the hydrogen in their core at the end of the main sequence, stars with initial masses in the range $8-40 M_{\odot}$ become large and cool Red Supergiants. When they leave the Red Supergiant branch, those stars evolve via the Yellow Hypergiant phase, followed by the Luminous Blue Variable phase (LBV), to finally become Wolf-Rayet stars (Oudmaijer et al., 2009). The stellar winds associated with these phases, followed by a final supernova explosion, are essential for the chemical enrichment of galaxies and provide kinetic energy that can trigger star formation. These stellar winds are likely due to a combination of pulsation and radiation pressure on dust. This leads to the formation of a dusty circumstellar envelope which makes post-main sequence objects bright infrared sources.

As part of a mid-infrared imaging survey of evolved stars (Lagadec et al. 2011), we observed the very bright mid-infrared source (with a $12 \mu\text{m}$ flux $F_{12}=1243$ Jy) IRAS 17163-3907 (hereinafter IRAS17163).

IRAS 17163 (a.k.a. Hen 1379) was discovered by Henize in 1976 during a survey of emission line stars in the southern sky. From their $2.2 \mu\text{m}$ mapping (Valinhos $2.2 \mu\text{m}$ survey), Epchtein et al. (1987) classified this object as a PPN candidate. Optical spectra of this object allowed us to show that the distance to this object is four times larger than previously assumed, and thus too bright to be a post-AGB star.

We report here the direct detection of a double detached shell around the central star of this post-Red Supergiant object.

2. Observations and data reduction

We observed IRAS17163 in the mid-infrared with VISIR on the VLT (Lagage et al., 2004) with 3 filters: PAH1 ($8.59 \mu\text{m}$, half bandwidth $0.42 \mu\text{m}$), SiC ($11.85 \mu\text{m}$, $2.34 \mu\text{m}$) and NeII ($12.81 \mu\text{m}$, $0.21 \mu\text{m}$). We used the imager in burst mode, using a pixel scale of 0.075 arcsec and a field of view of 19.2×19.2 arcsec. With the burst mode, all the chopping and nodding images are recorded, allowing the reconstruction of quality-enhanced images using shift and add techniques. We used the standard chopping/nodding technique to remove the background. We shifted and added the images using a maximum of correlation algorithm, after removing the bad images. Our observations were obtained during one of the driest nights ever in Paranal (0.43 mm of precipitable water vapor in the atmosphere). The quality of mid-infrared data being mostly affected by humidity, we obtained diffraction-limited images with a great stabil-

* Based on observations made with the Very Large Telescope at Paranal Observatory under program 081.D-0130(A).

** Based on observations made with the Mercator Telescope, operated on the island of La Palma by the Flemish Community, at the Spanish Observatorio del Roque de los Muchachos of the Instituto de Astrofísica de Canarias.

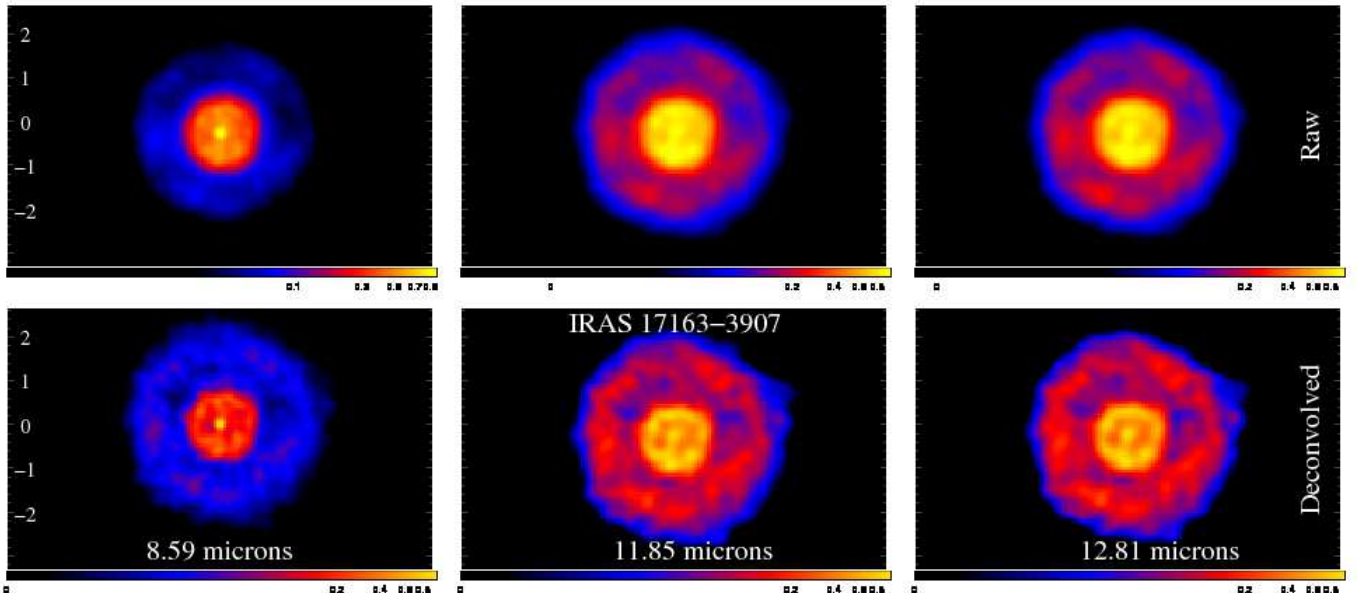


Fig. 1. VISIR/VLT mid-infrared images of IRAS 17163 at different wavelengths. The raw and deconvolved images are displayed for each filter. North is up and East left. The spatial scale is in arcsec and the intensity scale indicates the relative intensity. We clearly see the central star and two dusty detached shells.

ity (seeing+sky background) throughout the whole observing run. The images were deconvolved using the standard star HD 163376 as a measure of the Point Spread Function (PSF, observed before and after the science target with the same integration time of 30 seconds) and a maximum of likelihood algorithm with 50 iterations. Fig. 1 shows the raw and deconvolved images in the three filters.

We obtained an optical spectrum of IRAS 17163 using the HERMES instrument (High Efficiency and Resolution Mercator Echelle Spectrograph; Raskin et al., 2011) on the Mercator telescope (1.2 m) in La Palma. HERMES is a high-resolution fiber-fed echelle spectrograph offering a spectral resolution $R \sim 80\,000$ and a 2.54 arcsec field of view. We obtained 4 exposures of 1200 seconds each, under mediocre seeing conditions, resulting in a SNR of 20 at 6000 \AA . The pipeline-reduced spectrum stretches from 3770 to 9900 \AA , but due to the red nature of the source, it only appears above the noise from 5300 \AA onwards.

3. A new Post-Red Supergiant star

Diffuse interstellar Bands (DIBs), due to absorption by the interstellar medium, are seen in our optical spectrum of IRAS 17163. This allows us to estimate the distance to the observed object.

We adopted the relation defined by Reid et al. (2009) to calculate the kinematic distances for interstellar clouds observed in the line-of-sight toward IRAS 17163. The $K\text{ I}$ doublet velocity profile is plotted in Fig. 2. Three main interstellar velocity components are observed at local standard of rest (LSR) velocities of -31.7 , -10.1 , and 5.9 km s^{-1} . A possible weak component at -58.5 km s^{-1} is seen in both KI profiles. In addition, we observe narrow (FWHM $\sim 0.15 \text{ \AA}$) interstellar C_2 absorption lines at a LSR velocity of -32.3 km s^{-1} .

For the interstellar cloud at $\sim -32 \text{ km s}^{-1}$ we obtain the strongest constraints on the kinematic distance. We find a lower limit of 3.6 kpc for this interstellar cloud, which is also a lower limit of the distance to IRAS 17163.

If the Galactic rotation model is applied to the component at 5.9 km s^{-1} this would give a *lower* limit of $17.4^{+1.84}_{-1.33}$ kpc to the star. This, however, is incompatible with the inferred total

Table 1. Measured DIB strengths (in \AA , with 10% uncertainties) towards IRAS 17163. The 8621 \AA DIB appears blended with a H I emission line and was thus rejected for the calculation of $E(B-V)$. $\text{EW}/E(B-V)$ are taken from Luna et al. (2008).

DIB	EW (\AA)	EW/ $E(B-V)$	$E(B-V)$ for IRAS 17163
5780	0.91	0.46	1.98
5797	0.48	0.17	2.82
6379	0.14	0.088	1.59
6613	0.404	0.21	1.92
8621	0.497	0.37	1.34

line-of-sight reddening. We consider it most likely that this diffuse cloudlet has a peculiar velocity with respect to the rotational/radial velocity of the Galactic disk in this direction. The weak K I cloud at -58.5 km s^{-1} would correspond to a minimum distance of 4.7 kpc.

The K I velocity absorption profile is shown together with both the Galactic radial velocity (in LSR) and the visual extinction A_V as a function of distance.

From the measured equivalent widths for the 5780, 5797, 6379, and 6613 \AA DIBs we infer a reddening, $E(B-V)$, between 1.6 and 2.8 mag (Luna et al., 2008), with a mean of 2.1 mag (Table 1). For typical ISM dust, the total-to-selective visual extinction is $R_V = 3.1$ (Fitzpatrick & Massa 2009) and leads to a visual extinction of 6.4 magnitudes. The maximum value for the reddening corresponds to $A_V \sim 8.7$ mag. In Fig. 2 we plot the visual extinction versus distance extracted from the 3D Galactic dust extinction map constructed by Drimmel et al. (2003). We also indicate the distances derived from interstellar visual extinction values of 6 and 9 mag towards IRAS 17163. Although the Galactic dust extinction model may not be entirely accurate for sightlines within ~ 20 degrees toward the Galactic center, in this case the different distance determinations are fully consistent with each other.

In conclusion, the strong interstellar component at -32 km s^{-1} and the observed visual extinction, $A_V \geq 6$ mag sug-

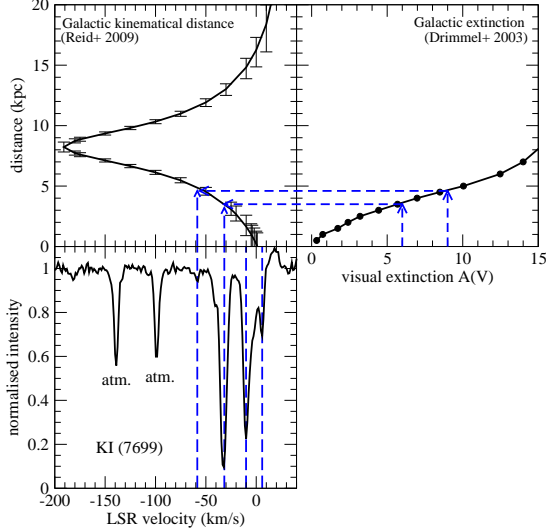


Fig. 2. The K₁ doublet velocity profile (lower left) of IRAS 17163, together with the Galactic kinematical distance estimate (upper left) from Reid et al (2009) and the model of Galactic extinction (upper right) from Drimmel et al. (2003). This indicate that the distance of IRAS 17163 is between 3.6 and 4.7 kpc.

gest a distance of 3.6 kpc to this IS cloud, and provide a lower limit to the distance of IRAS 17163. The maximum visual extinction (~ 9 mag) consistent with the measured DIBs strengths implies an upper limit to the distance of ~ 4.7 kpc. Therefore, the distance to IRAS 17163 is between 3.6 and 4.7 kpc.

This is four times further than what was previously assumed by Le Bertre et al. (1989), who classified this star as a post-AGB star. The luminosity of IRAS 17163 ($5 \times 10^5 L_{\odot}$, see Sect. 5.1) is thus well above the maximum luminosity of a post-AGB star ($\sim 10^4 L_{\odot}$; Schoenberner et al., 1983). IRAS 17163 is clearly not a post-AGB star, but very likely a post-Red Supergiant.

4. The double dust shell

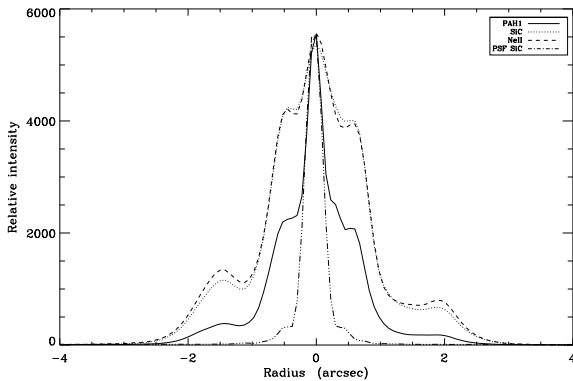


Fig. 3. Radial profile of the non deconvolved images in the three VISIR filters, showing the presence of the star and a double detached shell. The PSF is also shown for reference.

Le Bertre et al. (1989) obtained observations of IRAS 17163 and concluded that IRAS 17163 was located at 1 kpc from the

Sun, with a luminosity well below the maximum for post-AGB stars. The high polarization ($p \sim 12\%$) measured in V, R and I seems to indicate that the circumstellar envelope is highly aspherical. IRAS 17163 is unresolved in the optical images obtained with the ESO 1.5m danish telescope at la Silla (Chile), (Le Bertre et al., 1989), while infrared speckle interferometric observations indicate an angular dimension of $1.11 \pm 0.23''$ in L band ($3.6 \mu\text{m}$) (Starck et al., 1994). The high resolution H_{α} profile of IRAS 17163 indicate a wind velocity of $\sim 63 \text{ km s}^{-1}$.

IRAS 17163 was observed by the HST in the optical (Siódmiak et al., 2008), but classified as not resolved. The integration time was short (45s) and after inspection of the HST image, it appears that the dimension of the detached shells correspond to the Airy pattern of the HST at the observed wavelengths, which is why the authors did not see the detached shells (Siódmiak, private communication). The images of IRAS 17163 we obtained with VISIR are displayed Fig. 1. The object is clearly resolved in all the filters, with a diameter of $\sim 5''$. These are the first direct images of the circumstellar material around this very bright infrared source. The mid-infrared morphology of IRAS 17163 is similar to a fried egg, and we dubbed it the "Fried Egg" nebula. The object is circular at large scale and the central star can be observed in all the filters.

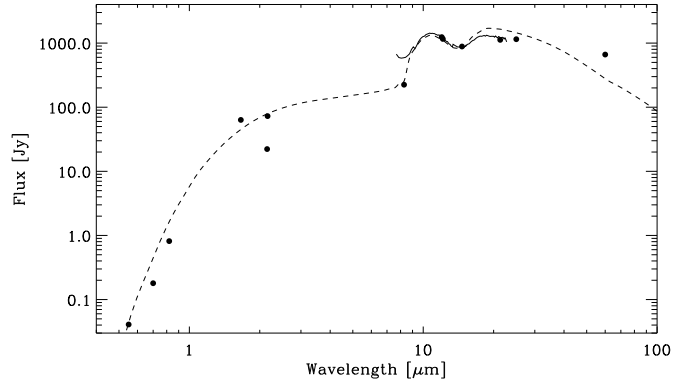


Fig. 4. Spectral energy distribution of IRAS 17163, the data points are from Szczerba et al., 2007. The dashed line represents our best radiative transfer model fit to the data.

The most striking aspect of these images is the presence of a double detached shell around the central star. This is more clearly seen in Fig.3 which shows a cut along the North-South direction in the three deconvolved images. We can clearly see two shells at ~ 0.6 and $1.5''$ from the central star. The images show that those shells are quite round. The shells however show some clumpy structures that are apparent in all the images and are thus not deconvolution artifacts. While on the raw images, the shells seems to be very smooth, the deconvolved images clearly show that these shells are made of a large number of clumps. We can also see a large hole in the second dusty shell along a P.A. of $\sim 45^{\circ}$. An extended structure, which seems to link the central star and the first shell is also seen along a P.A. $\sim 170^{\circ}$. There are some signs for a departure from spherical symmetry in the core of the nebula.

Considering a distance to the object of 4 kpc, the two shells have a radius of 2400 and 6000 A.U. respectively. Assuming a distance of 4 kpc and an expansion velocity of 40 km s^{-1} , this leads to an estimate of ~ 435 years for the time interval between the two shells.

To estimate the amount of dust present in the observed shells, we developed a radiative transfer model. We used the code described by Szczerba et al. (1997). The aim of our model is to fit both the SED and the intensity profile in our three VISIR images to get an estimate of the mass of dust in the envelope. The IRAS spectrum of IRAS 17163 shows the presence of silicate features, indicating that O-rich dust is present in the circumstellar envelope. Assuming a distance of 4 kpc, a star effective temperature of 8000 K and that the dust is made of circumstellar silicates with a standard MRN size distribution (Mathis et al., 1997), we obtained the best fit to the SED and radial dust distribution with a total dust mass of $0.04 M_{\odot}$, and a mass-loss rate varying with r^{-1} between the shell, as the SED could not be fitted without the presence of dust in between the shells. Assuming a lower limit of 100 for the gas-to-dust mass ratio, this leads to a total gas mass of $4 M_{\odot}$ in the ejecta and an average mass-loss rate of $10^{-4} M_{\odot} \text{yr}^{-1}$ and $2-3 \times 10^{-3} M_{\odot} \text{yr}^{-1}$ associated with the formation of the inner and outer shells respectively. Some dust is present in the inter-shell, and the presence of hot dust (~ 1500 K) close to the central has to be assumed to reproduce the flux of the central unresolved source. In the first shell the mean dust temperature ranges from 230 to 180 K, while in the outer shell it ranges from 150 to about 110 K. Assuming a width of 0.5 arcsec for each shell, we found that 0.002 and $0.005 M_{\odot}$ of dust are present in the inner and outer shells respectively.

5. Discussion

5.1. A Yellow Hypergiant

The optical spectrum of IRAS 17163 shows the presence of the 7450 \AA NI line and the absence of Helium lines, which indicates that the central star is either a late B or early A central star (Gray & Corbally, 2009), with an effective temperature in the range 7500-10000 K. If we assume, as estimated by the DIBs and the K I radial velocity we observed (Sect.3), a distance of 4 kpc for the object, its luminosity (measured by integrating the SED, (Fig. 4)) is $\sim 5 \times 10^5 L_{\odot}$. If one compares the location of IRAS 17163 on a temperature-luminosity diagram (Fig. 5), as the one presented by Oudmaijer et al.(2009), we can see that its properties are very similar to the brightest Yellow Hypergiants like the famous IRC+10420, with its temperature and luminosity just below the Luminous Blue Variables (LBVs).

5.2. Mass-loss variations

Yellow Hypergiants are not in a quiet evolutionary phase (Oudmaijer, 2009) and display episodic ejections, moving alternatively from the blue to the red on an HR diagram. The two detached shells we observe are likely due to such events. HST imaging of the Yellow Hypergiant IRC +10420 has shown the presence of partial shell and knot structures, which represent episodic ejection events (Tiffany et al. 2010, and references therein). We observed two shells due to phases of enhanced mass-loss separated by ~ 400 years. The central stellar source in the 10-micron image cannot be fitted with a stellar SED, which could be due to hot dust close to the star, indicating the presence of a third, unresolved shell next to the central star. The presence of clumps of dust close to the central star could explain the polarization observed for IRAS 17163. The unusual high linear polarization could also be partly due to alignment of interstellar grains in this line of sight. Polarization measurements of field stars near IRAS 17163 would be needed to resolve this issue. It is possible that many other shells are present further away from the central star. Such shells are not observed because of the small field of

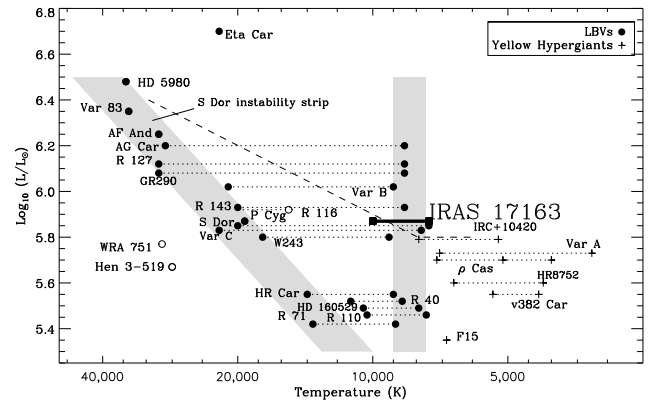


Fig. 5. Temperature-luminosity diagram of post-Red Supergiants, showing that IRAS 17163 is likely to be a Yellow Hypergiant. The grey bands on the left and right of the diagram represent respectively the regimes in the HR diagram which the LBVs occupy when they are in the quiescent phase (left) and the active phase (right) at maximum visual brightness (Smith et al. 2004.)

view of VISIR, the fact that these shells would be less dense and thus weaker and/or the fact that dust further away would be colder and thus emit at longer wavelengths. Such shells would explain the discrepancy between our radiative transfer model and the observed flux at 60 microns. Millimeter observations of the Fried Egg should allow the detection of such shells.

6. Conclusions

We presented the first resolved images of IRAS 17163. The morphology we observed led us to dub this object the ‘‘Fried Egg’’ nebula. We resolved two large concentric spherical dusty shells around the central star, itself embedded in dust. More than $4 M_{\odot}$ of gas and dust have already been ejected by the star. IRAS 17163 was previously classified as a post-AGB star, but the presence of DIBs in the optical spectra we obtained led us to the conclusion that the object is four times further than previously suggested and is thus a post red supergiant. The location of the Fried Egg on an HR diagram and the remarkable similarity between its optical spectra and the one of the prototype Yellow Hypergiant IRC +10420 indicate that the Fried Egg is probably a Yellow Hypergiant. The presence of detached shells around IRAS 17163 is a confirmation that non quiescent mass-loss occurs during this phase of stellar evolution.

Acknowledgements. The authors would like to thank the anonymous referee for providing us with constructive comments and suggestions.

References

- Drimmel, R., Cabrera-Lavers, A., & López-Corredoira, M. 2003, *A&A*, 409, 205
- Epchtein, N., Le Bertre, T., Lepine, J. R. D., et al. 1987, *A&A SS*, 71, 39
- Fitzpatrick, E. L., & Massa, D. 2009, *ApJ*, 699, 1209
- Gray, R. O., & Corbally, C., J. 2009, Princeton University Press, 2009
- Henize, K. G. 1976, *ApJS*, 30, 491
- Lagadec, E., et al. 2011, arXiv:1102.4561
- Lagage, P. O., et al. 2004, *The Messenger*, 117, 12
- Le Bertre, T. et al. 1989, *A&A*, 225, 417
- Luna, R. et al., 2008, *A&A*, 480, 133
- Mathis, J. S., Rumpl, W., & Nordsieck, K. H. 1977, *ApJ*, 217, 425
- Oudmaijer, R. D. et al., 2009, *The Biggest, Baddest, Coolest Stars*, 412, 17
- Raskin, G., et al. 2011, *A&A*, 526, A69
- Reid, M. J., et al. 2009, *ApJ*, 700, 137
- Schoenberner, D. 1983, *ApJ*, 272, 708
- Siódmiak, N. et al., & Szczerba, R. 2008, *ApJ*, 677, 382

- Smith, N., Vink, J. S., & de Koter, A. 2004, *ApJ*, 615, 475
Starck, J.-L., Bijaoui, A., Lopez, B., & Perrier, C. 1994, *A&A*, 283, 349
Szczerba, R., Omont, A., Volk, K., Cox, P., & Kwok, S. 1997, *A&A*, 317, 859
Szczerba, R. et al. 2007, *A&A*, 469, 799
Tiffany, C., Humphreys, R. M., Jones, T. J., & Davidson, K. 2010, *AJ*, 140, 339